Journal of The Electrochemical Society, **151** (1) A23-A30 (2004)
0013-4651/2003/151(1)/A23/8/$7.00 © The Electrochemical Society, Inc.

Vinylene Carbonate and Li Salicylatoborate as Additives in $LiPF_3(CF_2CF_3)_3$ Solutions for Rechargeable Li-Ion Batteries

D. Aurbach,[a,*,z] J. S. Gnanaraj,[a] W. Geissler,[b] and M. Schmidt[b]

[a]*Department of Chemistry, Bar-Ilan University, Ramat-Gan 52900, Israel*
[b]*Merck KGaA D-64293 Darmstadt, Germany*

Merck KGaA developed $LiPF_3(CF_2CF_3)_3$, (LiFAP) as a new electrolyte that can replace the commonly used $LiPF_6$ in Li-ion batteries. Vinylene carbonate and Li salicylato borate (Merck's AD25) were studied as additives for LiFAP solutions in mixtures of ethylene, dimethyl, and diethyl carbonates with composite graphite and $LiMn_2O_4$ electrodes. The tools for this study included voltammetry (fast and slow scan rates), chronopotentiometry, impedance spectroscopy, electron microscopy, Fourier transform infrared spectroscopy, and X-ray photoelectron spectroscopy. It was found that LiFAP solutions containing VC were superior for both graphite and $LiMn_2O_4$ (spinel) electrodes. The effect of additives on the electrodes' performance can be clearly attributed to their impact on the surface chemistry of these electrodes.
 [DOI: 10.1149/1.1631820]

Manuscript submitted March 17, 2003; revised manuscript received July 15, 2003. Available electronically November 21, 2003.

The increasing demand of power sources for portable equipment and electric vehicles has intensified efforts to develop rechargeable lithium batteries with high power density and rapid rechargeability. The most common Li-ion batteries comprise lithiated graphite anodes, $LiCoO_2$ (composite) cathodes, and electrolyte solutions based on $LiPF_6$ salt in organic carbonate solvents.[1]

In general, both the solvent molecules and the PF_6^- anions are reduced on the Li-C electrodes to form surface films comprising $ROCO_2Li$, ROLi, and Li_2CO_3, species containing Li-C bonds, polymeric species (*e.g.*, polycarbonate, polyethylene), LiF, Li_xPF_y, and Li_xPOF_y species.[2] These films passivate the Li-C electrode and lead to their apparent (kinetically controlled) stability in solutions. Also, surface films are formed on $LiMO_2$ cathodes in these solutions (M = V, Co, Mn, etc).[3] The performance of the cathodes is also largely influenced by surface phenomena.[4] $LiPF_6$ was chosen to be the commercially used electrolyte for Li-ion batteries only because other available salts are worse (for example: $LiClO_4$ is explosive, and $LiAsF_6$ is excluded due to the arsenic). $LiPF_6$ itself always brings with it HF contamination, which is detrimental to the performance of both negative and positive electrodes.[5] There is a pronounced difference in the surface chemistry of the negative and the positive electrodes in Li-ion batteries. In the case of the Li-C electrodes there is a constant driving force for the reduction of solution species, and hence, their passivation phenomena are driven by electrochemical (cathodic) reactions. In the case of cathodes, there is no major electrochemical reactivity of the solutions at the usual maximal charging potential of the cathodes ($E < 4.2$-4.3 V *vs.* Li/Li^+). The major possible surface reactions of the cathodes are driven by chemical properties. For instance, HF reacts with the $LiMO_2$ cathode materials to form surface LiF, and some of the cathode materials, *e.g.*, $LiNiO_2$, are nucleophilic and attack the electrolytic alkyl carbonate molecules, thus forming $-OCO_2Li$ surface groups and/or inducing polymeric species such as polycarbonates.[6] It should be noted that the capacity fading found for both Li-C and $LiMO_2$ electrodes in Li-ion batteries is largely due to surface phenomena related to the above reactions. Surface film formation may increase the electrodes' impedance and even isolate electrically part of the active mass. At elevated temperatures, the above-described surface phenomena occur even more intensively; higher electrode impedance may be developed, and pronounced surface-related capacity fading of Li-ion electrodes can be observed.

Major challenges in Li-ion battery technology relate to the improvement of high temperature and high rate performance and to minimizing capacity fading during prolonged operation. There are attempts to replace the $LiCoO_2$ cathode materials of the present Li-ion batteries with less expensive and more environmentally friendly materials such as $LiMn_2O_4$ (spinel) and its derivatives,[7] $LiNi_{1-x}M_xO_2$, or $LiFePO_4$ (olivine).[8] The stability of $LiMn_2O_4$-based electrodes, as well as their capacity-fading mechanisms (*e.g.*, Mn-ion dissolution, Jahn-Teller distortion, formation of defects) in Li-ion battery electrolyte solutions, have been explored extensively in recent years.[9-12] Poor performance at elevated temperature is a crucial problem of $LiMn_2O_4$ electrodes.[13]

In the last decade, various attempts have been made to develop appropriate electrolytes that are chemically and electrochemically stable in the presence of strong oxidizing cathode materials such as $LiCoO_2$, $LiMn_2O_4$, and $LiNiO_2$, and the strong reducing Li-C materials. For instance, $LiN(SO_2CF_3)_2$,[14] $LiC(SO_2CF_3)_3$,[6] $LiN(SO_2C_2F_5)_2$,[15] and Li-bis(oxalato)borate (LiBOB)[16] have been explored. In addition, there is an increasing number of reports on modification of electrolyte solution properties with a small amount of reactive additives whose presence in the Li-ion batteries improves the performance. As examples, CO_2,[17] SO_2,[18] alkyl or aryl sulfites,[19] vinylene carbonate (VC),[20] can be mentioned as additives that improve the performance of Li-ion battery systems.

Recently, we reported on the electrochemical performance of Merck's solutions containing a new salt, $LiPF_3(CF_2CF_3)_3$, (LiFAP).[21,22] It was proven that both Li-graphite anodes and $LiMn_2O_4$ cathodes perform better in LiFAP solutions than in the commercially used $LiPF_6$ solutions. In the present study, we have explored the effect of the VC and Li bis(salicylato)borate (Merck's AD25) additives in LiFAP solutions on the performance of graphite and $LiMn_2O_4$ spinel electrodes. Standard electrochemical techniques have been used in conjunction with surface sensitive techniques such as Fourier transform infrared (FTIR) and X-ray photoelectron spectroscopy (XPS).

Experimental

All the work was performed under a highly pure argon atmosphere in standard glove boxes from VAC Inc. The anodes were composed of synthetic graphite (KS-6) from Timrex Inc. (specific surface area of *ca.* 20 m^2/g, average particle size *ca.* 6 μm, 90 wt %), poly(vinyledene fluoride) (PVdF) binder (10 wt %) from Solvey Inc., and copper foil current collectors. The cathodes were comprised of $LiMn_2O_4$ powder (stoichiometric) from Merck KGaA (specific surface area of *ca.* 3 m^2/g, particle size of 5-10 μm, 75 wt %), 15 wt % graphite powder KS-6 (Timrex Inc.) as a conductive additive, 5 wt % PVdF, 5 wt % conductive carbon black, and an aluminum foil (Goodfellow, England) current collector. Slurries containing the active mass (2-10 mg depending on the type of experiment) and the binder were prepared using N-methyl pyrrolidone (Fluka Inc.) and were coated on the appropriate current collectors, as

* Electrochemical Society Active Member.
z E-mail: aurbach@mail.biu.ac.il

already described.[6] The electrodes were dried in an oven at 140°C and were then transferred to the glove boxes. LiFAP, LiFAP + 5% VC, and LiFAP + 1% AD25 1 M solutions in mixtures of ethylene carbonate-diethylcarbonate-dimethyl carbonate (EC-DEC-DMC, 2:1:2 by volume) were obtained from Merck KGaA (highly pure, Li battery grade) and could be used as received. The HF and water content in these solutions were at the ppm level, as measured at Merck. The electroanalytical characterizations of the electrodes were performed either in three-electrode cells based on standard coin-type cells[23] (model 2032, NRC Canada, ϕ 19 mm), or parallel plate cells made of polyethylene frames. In the coin cells, a Li wire reference electrode was pasted on a nickel wire, which was placed between the working electrode and the Li counter-electrode foil, covered by separator foils (Celgard 2400). In the polyethylene cells, the working electrode (WE) was surrounded symmetrically on both sides by a Li counter electrode foil (mass of *ca.* 200 mg and surface area of *ca.* 4.65 cm^2). A Li wire (ϕ 1 mm) reference electrode was placed close to the WE. The solution volume in those cells was around 3 mL (low surface-to-volume ratio). Long-term cycling tests with graphite and $LiMn_2O_4$ electrodes were performed in two-electrode standard coin-type cells (using a porous polypropylene separator, Celgard Inc.). Those cells were hermetically sealed in a dry air-filled glove box using the 2325 coin cell crimper system from NRC/ICPET, Canada.

Freshly prepared graphite electrodes usually had an open circuit potential (OCP) of *ca.* 3.3 V (*vs.* Li/Li^+). They were aged by voltammetric cycling between 3.0 and 0. V (*vs.* Li/Li^+) at $\nu = 1$ mV/s (three cycles) before further studies.

Freshly prepared, thin $LiMn_2O_4$ electrodes with open circuit voltage OCV around 3. V (*vs.* Li/Li^+) were initially cycled four times (voltammetry) between 3.5 V and 4.25 V (*vs.* Li/Li^+) at 1 mV/s before the rigorous electrochemical measurements were made. Prolonged galvanostatic cycling of all the various cells was performed at C/10 or C/4 rates in coin-type cells at 30°C in an incubator (Carbolite Inc., model PIF30-200) and at 60°C in a homemade thermostat. For voltammetric measurements, an Arbin Inc. computerized multichannel battery tester and a computerized EG&G model 273 potentiostat were used. A Maccor multichannel system (model 2000) was used for prolonged galvanostatic cycling.

For surface analysis studies, we used a Magna 860 (Nicolet) FTIR spectrometer placed in a glove box under H_2O and CO_2-free atmosphere (fed by compressed air, treated with a Balston Inc., model A-05881 air purifier). The electrodes were analyzed after electrochemical studies by diffuse reflectance mode (a DRIFT accessory from Harrick Inc.), as already reported.[6] XPS characterization of electrodes was performed using an AXIS HS XPS spectrometer from Kratos Analytical Inc. (England). The samples were transferred from the glove boxes to the spectrometer by a homemade transfer system that included a gate valve and a magnetic manipulator from Norcal Inc. (USA). This system ensures full protection from exposure to atmospheric contaminants. We also characterized surface films formed on gold mirrors and Pt foils that were polarized to low or high potentials in the various solutions, by FTIR (external reflectance mode)[24] and XPS.

Impedance spectra were measured using the Autolab model PGSTAT20 electrochemical system and a frequency response analyzer from Eco Chemie B.V. Inc., driven by a Pentium II IBM PC. The amplitude of the *ac* voltage was 3 mV, and the electrodes were measured at a constant base potential after the appropriate equilibration, as already described.[6] Scanning electron microscope (SEM) measurements were performed with a JSM 840 scanning electron microscope (JEOL Inc.).

Results and Discussion

Graphite electrodes.—Figure 1 shows the first three cyclic voltammograms (CVs) of graphite electrodes cycled at the scan rate of 1 mV/s in LiFAP (additive free), LiFAP with VC and AD25 solutions. Those CVs reflect the irreversible reduction of solution species at potentials below 1.6 V, which formed passivating surface films (appearing only during the first cathodic wave), and the reversible lithium insertion and deinsertion processes at potentials below 0.20 V (cathodic) and above 0.15 V (anodic), respectively. Note that for each solution, the first cathodic wave looks different, reflecting the effect of the additives on the electrodes' surface chemistry. For instance, the first CV related to the LiFAP solution with AD25 (Fig. 1c) shows a pronounced irreversible cathodic peak around 830 mV, which should be attributed to reduction of the AD25 anion.

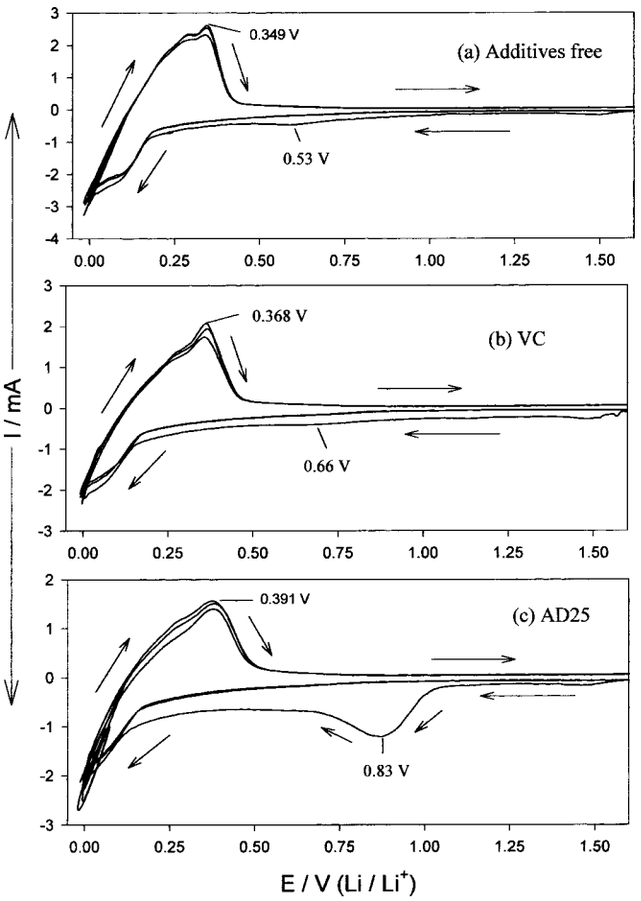

Figure 1. First three cyclic voltammograms between OCV and 0 V (Li/Li^+) at 30°C with graphite electrodes at the scan rate of 1 mV/s (lithium foil counter and reference electrodes). EC:DEC:DMC, 1 M (a) LiFAP, (b) LiFAP + 5% VC, and (c) LiFAP + 1% AD25 solutions, as indicated.

Figure 2 shows families of Nyquist plots measured at 30°C at different equilibrium potentials (indicated) with stabilized graphite electrodes during lithium insertion in the three solutions (additive-free, VC- and AD25-containing LiFAP solutions, respectively). The spectra include a high frequency, flat semicircle, another medium frequency feature which also looks like a small, flat semicircle, and a straight, steep Z'' *vs.* Z' response at the low frequencies. The high frequency semicircle relates to the surface films, which cover the graphite electrodes and are formed at low potentials by reduction of solution species.[2]

The semicircle reflects charge transfer resistance to Li-ion migration through the surface films, coupled with surface film capacitance. We attributed the feature appearing at the medium frequencies (very flat small semicircle) to charge transfer across the surface film-active mass interface, coupled with the relevant interfacial capacitance.[25] The low frequency part of the spectra relates to solid-state diffusion and accumulation of Li in the host ($C_{int} = 1/z''\omega$ at $\omega \rightarrow 0$).[25] It is very significant that the high frequency semicircles

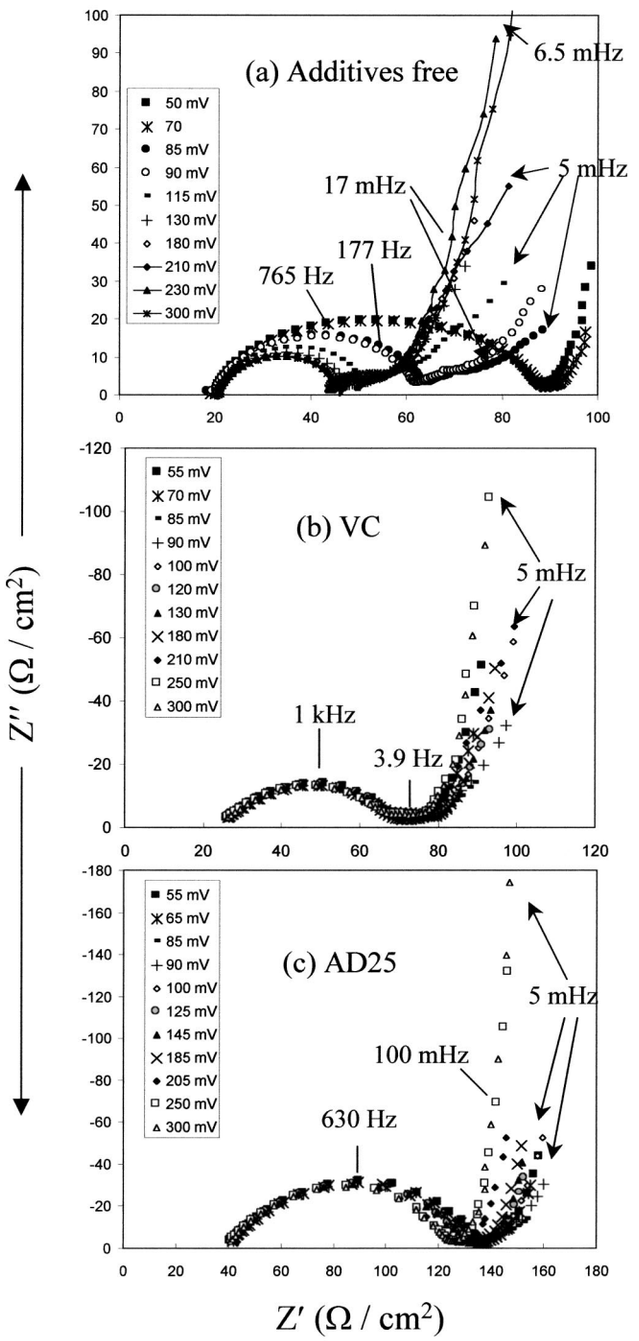

Figure 2. A family of Nyquist plots obtained from graphite (synthetic flakes KS6 from Timrex, Inc.) electrodes at different equilibrium potentials in EC-:DEC:DMC, 1 M (a) LiFAP, (b) LiFAP + 5% VC, and (c) LiFAP + 1% AD25 solutions, as indicated, at 30°C. These series of experiments were carried out after the electrodes were cycled (CV) in the potential range of interest, during which its surface chemistry was stabilized. Some frequencies are also marked near the spectra. The relevant potentials are indicated.

in the spectra measured with the additive-free solution were potential dependent (the semicircle increased as the electrodes reach the high intercalation stages, $LiC_{12} \rightarrow LiC_6$), while the high frequency parts of the spectra related to the solutions with the additives were nearly potential invariant. This may also show that the additives allowed formation of a stable passivation layer during the first cycle whereas it was not the case without additives, where passivation was completed during the 5-10 first cycles. This difference obviously reflects the strong impact of the additives on the surface films developed on the electrodes.

We suggest that the high frequency part of the impedance spectra of graphite electrodes may have changed as Li insertion progressed, because the surface films on the edge planes, through which Li ions were inserted, had to stretch due to the volume increase as stage 2 and stage 1 were reached,[26] when their transport properties may have deteriorated due to stress. Note that these changes are reversible, because the electrodes were measured after they were stabilized, and their protective surface films were fully developed. The fact that there was no significant change in the high frequency response of the impedance as a function of potential in the solutions containing VC and AD25 may indicate that the surface films formed on graphite in these systems were more flexible and better accommodating of the volume changes of the graphite particles, compared to the surface films formed in the additive-free solutions. This correlates well with our previous studies.

In LiFAP solutions, the surface films formed on graphite were dominated by species such as $(CH_2OCO_2Li)_2$ formed by reduction of EC.[22] Such species, being Li salts, cannot form overly flexible surface layers. There is also a significant difference in the real part (R) of the spectra presented, with $R_{VC} < R_{\text{no additive}} < R_{AD25}$ once the fully charged (lithiated) state is reached. Reduction of VC, as discussed earlier, forms polymeric species (*e.g.*, poly-Li alkyl carbonate species),[27] which should improve the mechanical properties of the surface films. Hence, the impedance spectra in Fig. 2b (VC solution), whose high frequency part is invariant with respect to the potential/Li insertion level, probably reflect the formation of unique surface films because of the impact of VC on the electrodes' surface chemistry, as already described.[27] The presence of AD25 also influences the electrodes' surface chemistry and seems to improve the passivation of the lithiated graphite electrodes. The way in which AD25 influences the surface chemistry of these electrodes is not yet fully understood.

Figure 3A shows typical curves of charge/discharge capacity *vs.* cycle number of graphite electrodes (*vs.* Li CE) at 30°C in coin-type cells at a C/10 rate for the first 5 cycles, and then at a C/4 rate for the rest of the experiments, in an additive-free solution and in solutions containing VC and AD25. The cells were cycled over 100 cycles and showed a steady capacity *ca.* 350 mAh/g. As seen in this figure, the stability of electrodes upon cycling in all three solutions was nearly the same. The irreversible capacity measured was the lowest in the additive-free solution (around 30%), compared to that of the other solutions containing VC or AD25 (40 and 45%, respectively). This may also indicate that the passivation was not fully achieved in the additives-free solution during the first cycle. The higher irreversible capacity measured in the solution containing additives reflects the reactivity of the additives toward the Li-C electrodes, which, on the one hand, drive them to react predominantly on the electrodes' surface, thus forming surface films, but on the other hand, cause a consumption of irreversible charge due to enhanced surface reactions.

Figure 3B shows typical curves of charge/discharge capacity *vs.* cycle number of graphite electrodes in coin-type cells at C/4 rates with the three solutions as indicated, at 60°C.

An obvious conclusion from these studies is that high stability and reversibility of graphite electrodes at elevated temperatures is obtained in the LiFAP-VC solutions.

Figure 4 shows SEM micrographs of a pristine graphite electrode and electrodes after cycling in the three solutions at 60°C, as indicated. The SEM image of the pristine electrode clearly shows the graphite flakes of a few μm of average size. The morphological features in Fig. 4b-d reflect the formation of surface films on these electrodes, mostly due to their intrinsic reactions with solution components. These films are characterized by a mosaic-like morphology composed of nanometric grains. Pronounced morphological changes and cracking due to cycling are seen in additive-free images (b) of electrodes cycled in the solution, compared with the smooth surface

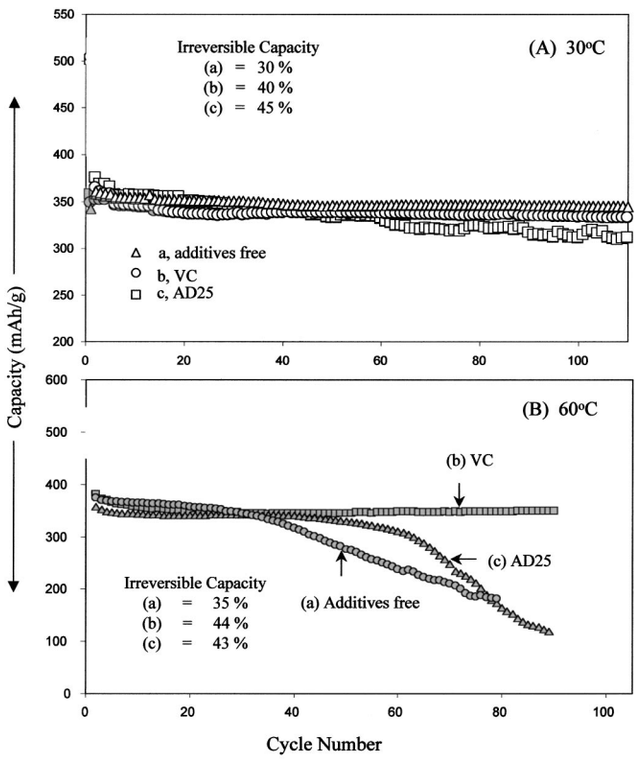

Figure 3. Typical cycle life curves (capacity *vs.* cycle number) of graphite electrodes obtained in coin-type cells. Li metal counter electrodes, EC:DEC:DMC, 1M (a) LiFAP, (b) LiFAP + 5% VC and (c) LiFAP + 1% AD25 solutions, as indicated in the figure. (A, Upper chart) 30°C, (B, lower chart) −60°C. The current rates for the charge and the discharge processes are C/10 for the first 5 cycles and the rest at C/4 testing at (A) 30°C and (B) 60°C.

morphology of electrodes cycled in VC-containing solutions. These morphological features presented in Fig. 4 correlate well with the improved performance of graphite electrodes in the VC-containing solutions (Fig. 3B).

In order to understand the surface chemistry of graphite electrodes, the electrodes were polarized to low potentials in the solutions, which determined their performance,[1-3] and we studied the surface chemistry by FTIR spectroscopy, using the diffuse reflectance mode. Figure 5a shows an *ex situ* FTIR spectrum of a pristine graphite electrode, and Fig. 5b shows a spectrum of an electrode polarized to 100 mV (*vs.* Li/Li^+) in a LiFAP solution for 3 h. The electrode was removed at 100 mV from the solution after the current decayed to a steady low value (close to zero). The spectra related to pristine graphite electrodes reflect the presence of some functional groups on their surfaces. These groups may include OH, C = O, or COOH. Spectrum 5b, related to the graphite electrode polarized to 100 mV, clearly reflects the surface films that cover the electrode. While the resolution of spectra measured from graphite electrodes is usually poor, due to the limitation of surface analysis by diffuse reflectance mode, spectrum 5b shows distinguishable peaks of $ROCO_2Li$ species at approximately 1640-1650 cm^{-1} (ν_{CO}), 1510-1550 (Li_2CO_3), 1450-1400 cm^{-1} (δ_{CH_2,CH_3}), and 850 (δ_{CO_3},$ROCO_2Li$).[28] The peaks at 1190 and 880 cm^{-1} belong to PVDF and Li_2CO_3, respectively. The δ_{CH_2} peaks at 1450-1400 cm^{-1} seem to be superimposed on the broad Li_2CO_3 peak (1520-1450 cm^{-1}).[28]

These spectral results further demonstrate what we previously found,[22] that in LiFAP solutions, the surface chemistry of graphite electrodes was dominated by reduction of the alkyl carbonate solvents ($ROCO_2Li$ formation by reduction of EC as a dominant sur-

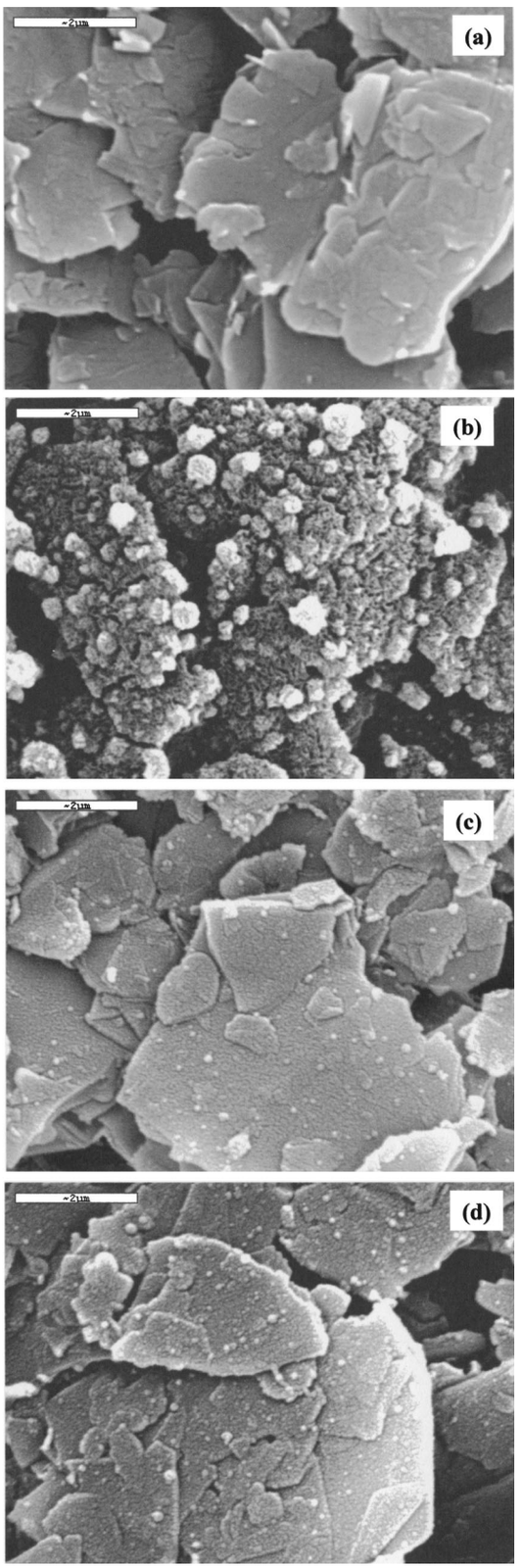

Figure 4. SEM micrographs of graphite electrodes (a) before and after cycling at 60°C in EC:DEC:DMC, 1 M (b) LiFAP, (c) LiFAP + 5% VC, and (d) LiFAP + 1% AD25 solutions. A scale (2 μm) appears in each picture.

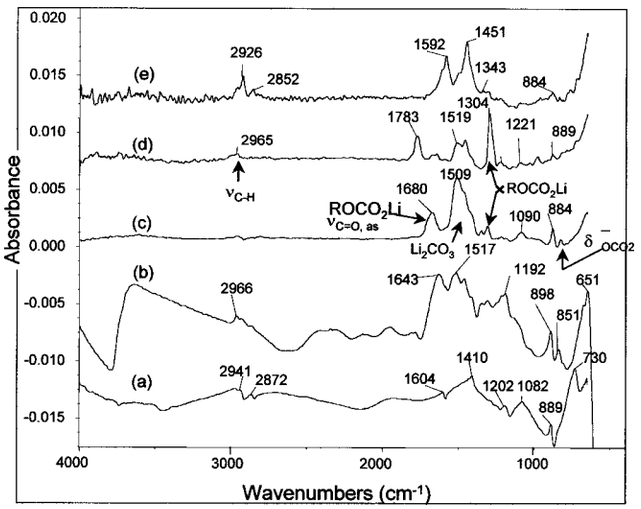

Figure 5. (A) FTIR spectra (diffuse reflectance mode) measured *ex situ* from (a) a pristine graphite electrode, (b) a graphite electrode polarized to 100 mV (*vs.* Li/Li^+) in an additive-free LiFAP solution, and FTIR spectra (grazing angle, reflectance mode) measured *ex situ* from reflective gold electrodes after being polarized cathodically to 300 mV *vs.* Li/Li^+ for 3 h in EC:DEC:DMC, 1 M (c) LiFAP, (d) LiFAP + 5% VC, and (e) LiFAP + 1% AD25 solutions.

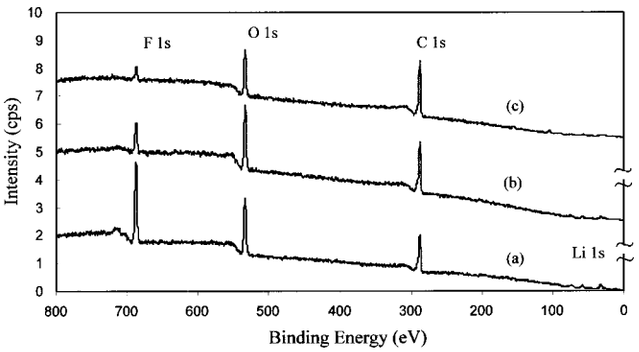

Figure 6. XPS data obtained from Pt electrodes polarized cathodically to 10 mV (for 3 h) in EC:DEC:DMC, 1 M (a) LiFAP, (b) LiFAP + 5% VC, and (c) LiFAP + 1% AD25 solutions.

face reaction[28]). This is in contrast to the case of $LiPF_6$ solutions, in which HF reactions and reduction processes related to the PF_6^- anion played an important role in determining the surface chemistry of graphite electrodes.[29] FTIR specta measured from graphite electrodes polarized in VC- and AD25-containing solutions were somewhat similar to spectrum 5b. The limited resolution of FTIR spectra measured from graphite electrodes does not allow us to determine the precise major impact of the additives on the graphite electrodes' surface chemistry. Hence, FTIR spectra were also measured from gold mirrors (*ex situ* external reflectance mode) polarized to low potentials in the three solutions. We know from previous studies[28] that the surface chemistry of carbon electrodes in polar aprotic Li salt solutions is similar to that of cathodically polarized noble metal electrodes in the same solutions. Spectra 5c-e belong to gold mirrors covered by surface films formed in additive-free, VC- and AD25-containing solutions, respectively. Spectrum 5c contains peaks of $ROCO_2Li$ and Li_2CO_3, as indicated, and hence, correlates with spectrum 5b (graphite), related also to the additive-free solution. Note the much better resolution of spectrum 5c. Such spectra were previously dealt with in depth[28,29] and are therefore not discussed again herein. They reflect the expected (similar) surface chemistry of graphite and noble metal electrodes in LiFAP/alkyl carbonate solutions.[22] It is very significant that spectra 5d and 5e related to the VC- and AD25-containing solutions are very different from spectrum 5c. These results clearly prove that the additives studied herein had a pronounced impact on the electrodes' surface chemistry. The spectra related to the VC-containing solution also had $ROCO_2Li$ peaks different from those of spectrum 5c, and a pronounced peak around 1780 cm^{-1}. We suggest that such a spectrum reflects the formation of VC reduction products that may include poly VC, polyethylene Li dicarbonate, other $ROCO_2Li$ species, and Li_2CO_3, as discussed earlier.[27] Spectrum 5e related to the AD25 solution shows pronounced peaks around 1590 and 1450 cm^{-1} that may be attributed to $-COOLi$ (carboxylate) groups.[30] These peaks may indicate that the AD25 is reduced via the B-O bonds to form carboxylates, which are derivatives of salicylic acid (AD25 is a compound of boron with two salicylates, which form an anion bound to Li^+).

Figure 6 compares XPS spectra of a Pt electrode polarized to low potentials (10 mV *vs.* Li/Li^+) in additive-free, VC- and AD25-containing solutions. The XPS spectrum related to the additive-free solution shows a higher fluorine content, compared to the spectra related to the additive-containing solutions. The carbon and oxygen peaks are characteristic of surface species comprising $ROCO_2Li$ and ROLi compounds, as discussed earlier.[27,29] Hence, these XPS spectra further demonstrate the strong impact of the additives on the electrodes' surface chemistry: their surface reactions dominate and suppress possible surface reductions related to the salt anion, which forms fluorine compounds (*e.g.*, LiF[22]).

$LiMn_2O_4$ (spinel) electrodes.—The behavior of $LiMn_2O_4$ spinel composite electrodes was also studied in the above electrolyte solutions. Figure 7 compares families of consecutive three CVs obtained from $LiMn_2O_4$ (stoichiometric) spinel electrodes cycled at different scan rates of 1 mV/s, 100 μV/s, and 10 μV/s in the three solutions (a-c). Each chart in Fig. 7, related to a specific scanning rate, compares CVs of identical electrodes in the three solutions. These CVs allow a qualitative comparison of the impact of the solutions on the electrodes' kinetics. The points of interest in this respect are the shape of the peaks, and the hysteresis between the corresponding redox peaks. As discussed earlier,[31] at the fast scanning rates (the mV/s domain), the CVs reflect the kinetics of charge transfer and solid state diffusion (Li-ions into the host). When the scanning rates are lower (the μV domain), the CVs reflect the thermodynamics of the system, *e.g.*, Li ordering via phase transitions. Fig. 7 shows that the CVs related to the additive-free solution are broader, with higher hysteresis, compared to those related to the additive-containing solutions.

Figure 8 shows families of Nyquist plots obtained by EIS measurements of $LiMn_2O_4$ electrodes in the three solutions, as indicated. The impedance spectra of these electrodes were previously discussed.[31,32] In brief, they reflected a serial nature of the Li insertion process that includes several stages: Li-ion transfer through surface films that may be formed on these electrodes (high frequency semicircle), interfacial charge transfer (medium-low frequency semicircle), solid state diffusion (a Warburg-type element), and accumulation (a steep Z'' *vs.* Z' response at the very low frequencies). All these elements indeed appeared in the spectra of Fig. 8. The impedance spectra presented are strongly dependent on the potential, as expected and discussed.[30,31] What is highly important for the present study is the pronounced impact of the presence of VC and AD25 on the spectra. It is clear from these measurements that both additives affected the electrodes' surface. They probably reacted on the surface of the active mass, thus affecting the interfacial charge transfer of the electrodes, and probably also their passivation and stability.

Figure 9A presents cycling data of $LiMn_2O_4$ electrodes at 30°C (repeated 100 galvanostatic delithiation/lithiation cycles at a C/10

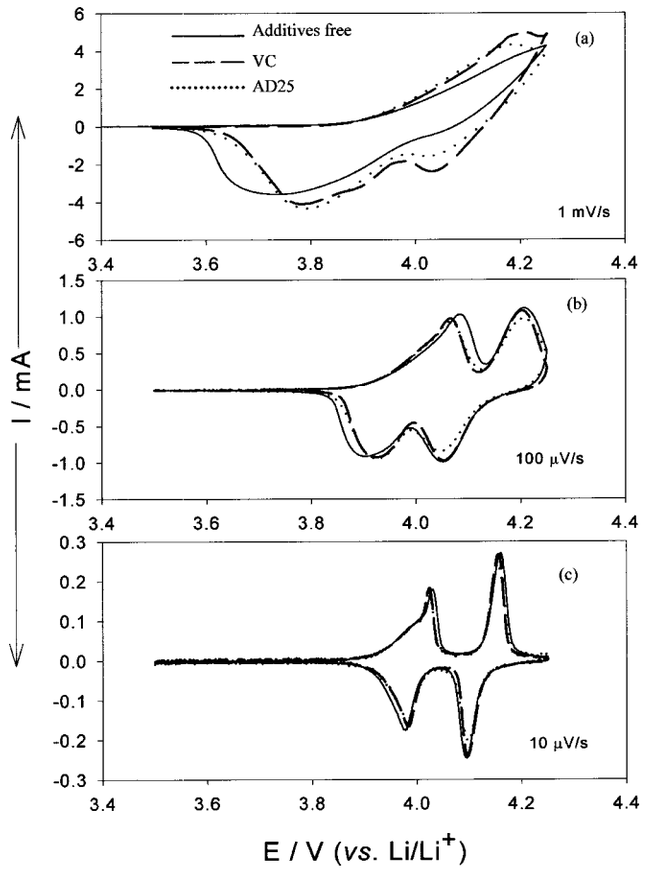

Figure 7. First three consecutive CVs of $LiMn_2O_4$ electrodes between 3.5 V and 4.25 V at a scan rate of (a) 1 mV/s, (b) 100 μV/s, (c) 10 μV/s (*vs.* Li/Li^+) (lithium as counter and reference electrodes) in EC:DEC:DMC, 1 M LiFAP (solid line), LiFAP + 5% VC (dashed line), LiFAP + 1% AD25 (dotted line), as indicated.

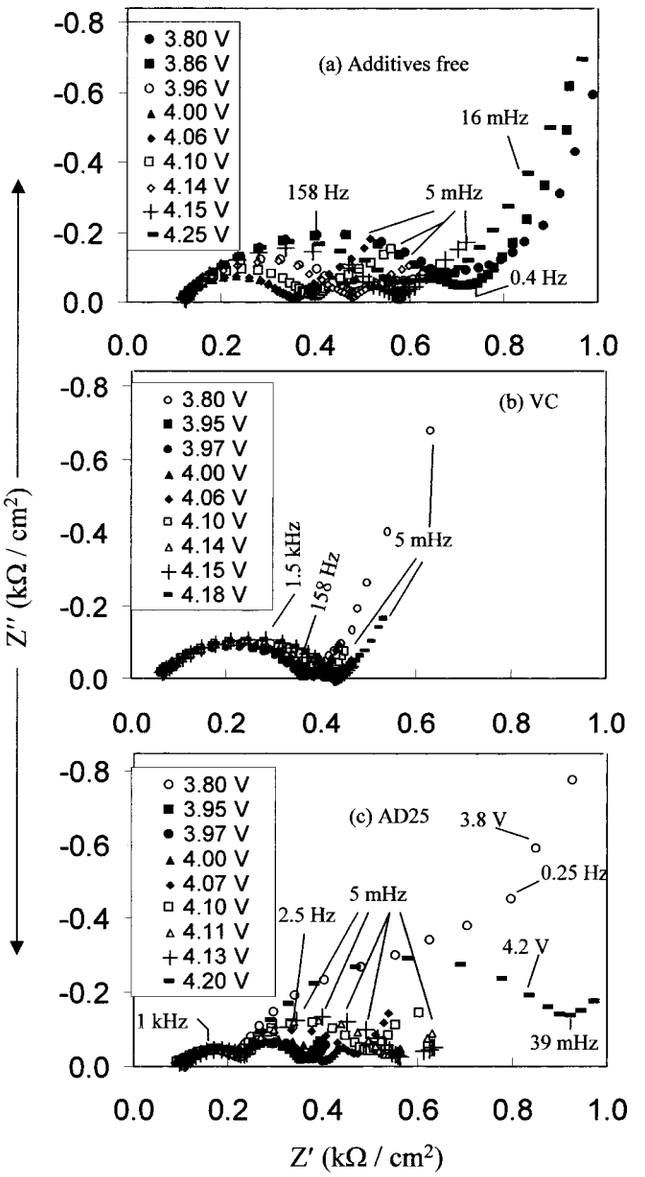

Figure 8. A family of Nyquist plots obtained from spinel, $LiMn_2O_4$ composite electrodes at different equilibrium potentials in EC:DEC:DMC, 1 M (a) LiFAP, (b) LiFAP + 5% VC and (c) LiFAP + 1% AD25 solutions, as indicated, at 30°C. That series of experiments were carried out after the electrodes were cycled (CV) in the potential range of interest, during which its surface chemistry was established. Some frequencies are also marked near the spectra. The relevant potentials are indicated.

rate for the first 60 cycles and then at a C/4 rate). As seen, the capacity and stability obtained for $LiMn_2O_4$ electrodes in additive-free and VC-containing solutions were higher than in the solution containing AD25. Figure 9B shows capacity *vs.* cycle number plots for $LiMn_2O_4$ electrodes at 60°C (100 repeated galvanostatic delithiation/lithiation cycling at a C/4 rate).

As expected, a fast capacity fading was observed at 60°C. Figure 9B demonstrates further that the solutions containing AD25 were inferior to the VC-containing or the additive-free solutions. The cycling experiments show that the VC solutions were superior, and the AD25 solutions inferior, as electrolyte solutions containing the relatively nonacidic LiFAP salt, for $LiMn_2O_4$ electrodes. The CV and electrochemical impedance spectroscopy (EIS) studies clearly indicate that the additives react on the $LiMn_2O_4$ surfaces, thus influencing their electrochemical performance. Possible surface chemistry effects of these solutions on $LiMn_2O_4$ cathodes were studied by FTIR and XPS techniques. In addition to measurements of $LiMn_2O_4$ electrodes after cycling, we measured the spectra of possible surface films formed on gold and platinum electrodes, polarized to 4.5 V (Li/Li^+) in the three solutions. The study of surface films formed on noble metals provides a better resolution of the spectral results, and hence, is a clue to understanding the more complex and less resolved spectra of the composite $LiMn_2O_4$ electrodes.

Figure 10 shows FTIR spectra obtained from gold mirrors (coated on glass), which were polarized anodically to 4.5 V in the three solutions, as indicated (*ex situ*, external reflectance mode).[29] All three spectra differ from each other and contain typical pronounced peaks of organic species around 2920-2850 cm^{-1} ($\nu_{C\text{-}H}$), 1800-1600 cm^{-1} ($\nu_{C=O}$), and 1450-1350 cm^{-1} ($\delta_{C\text{-}H}$). The peaks around 885-850 cm^{-1} may be attributed the species with P-F bonds. These spectra may reflect polymerization of the solvent molecules to derivatives of polyethylene oxide and polycarbonates, as already suggested.[33] The spectrum (Fig. 10b) related to the electrode polarized anodically in the VC-containing solution contains broad peaks around 1300-1200 and 1000-850 cm^{-1}, which do not appear in the other spectra, in addition to the peaks around 1800-1600 cm^{-1} ($\nu_{C=O}$), and 1500-1400 cm^{-1} (δCH_2). The electrode polarized anodically in AD25-containing solution is very rich in peaks, which appear around 2950-2900 cm^{-1} ($\nu_{C\text{-}H}$), 1820-1700 cm^{-1}, and with sharp peaks at 1612 ($\nu_{C\text{-}C}$, aromatic rings), 1484 ($\delta_{C\text{-}H}$) and 1350-

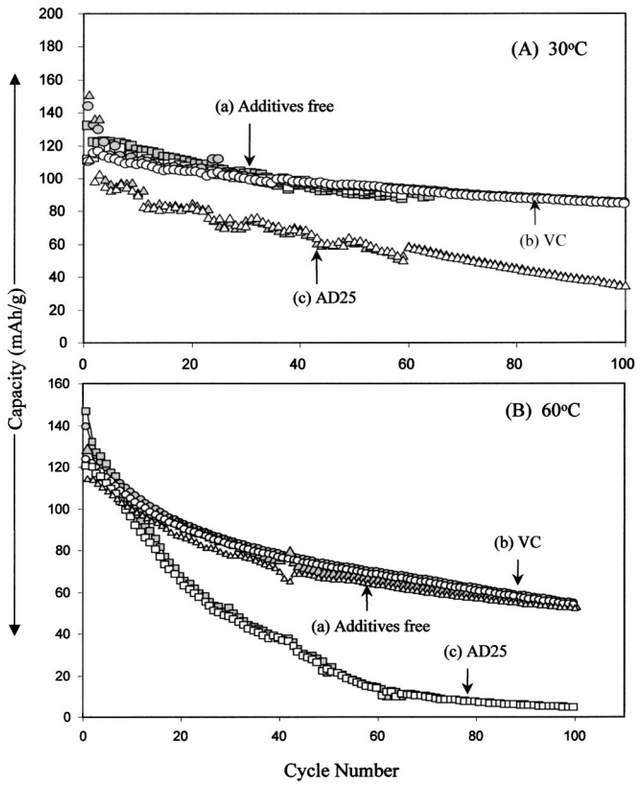

Figure 9. Typical cycle life curves (capacity *vs.* cycle number) of $LiMn_2O_4$ electrodes obtained at 30°C and at 60°C (9A and B, respectively) in coin-type cells (galvanostatic mode). Li metal counter electrodes, EC:DEC:DMC, 1 M (a) LiFAP, (b) LiFAP + 5% VC, and (c) LiFAP + 1% AD25 solutions, as indicated. The rates for charge and discharge at 30°C (9A) were C/10 for the first 50 cycles and the rest at C/4 and at 60°C (B) C/4 were C/4.

1250 cm^{-1} (δCH_3), 1100-1000 ($\nu_{C=O}$), and 770 cm^{-1}. These peaks may reflect surface species originating from some oxidation of AD25 to species containing derivatives of salicylic acids (esters, anhydrides). These spectral results are not sufficiently conclusive to allow us to elucidate exactly the surface chemistry developed on electrodes in these solutions, at high potentials. However, some useful information was obtained from them, namely, that it is clear that surface species can precipitate on electrodes at high potentials in all of these solutions. In addition, the pronounced difference among the

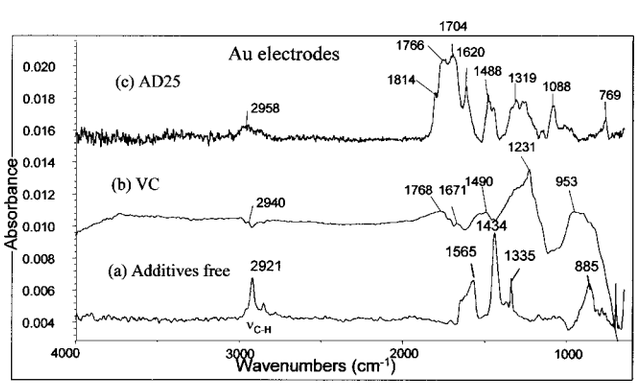

Figure 10. FTIR spectra (grazing angle reflectance mode) measured *ex situ* from reflective gold electrodes after being polarized anodically to 4.5 V *vs.* Li/Li^+ for 3 h in EC:DEC:DMC, 1 M (a) LiFAP, (b) LiFAP + 5% VC, and (c) LiFAP + 1% AD25 solutions.

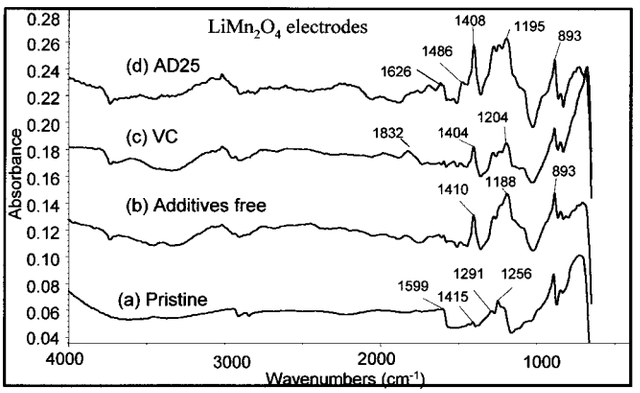

Figure 11. FTIR spectra (diffuse reflectance mode) measured *ex situ* from $LiMn_2O_4$ spinel electrodes (a) pristine electrode and (b-d), electrodes after cycling (CVs at 1 mV/s) *vs.* in EC:DEC:DMC, 1M (b) LiFAP, (c) LiFAP + 5% VC, and (d) LiFAP + 1% AD25 solutions.

spectra of Fig. 10 clearly demonstrate a pronounced impact of the VC and AD25 additives on the surface chemistry developed on electrodes at high potentials.

Figure 11 shows FTIR spectra of a pristine $LiMn_2O_4$ electrode and of $LiMn_2O_4$ electrodes after cycling in the 3-4.3 V potential range at 30°C in the three solutions, as indicated. The spectrum of the pristine electrode reflects the presence of a PVdF binder (*e.g.*, $\nu_{C=F}$ around 1200 cm^{-1}) and possible surface groups on the carbon additive. The spectra related to the electrodes after cycling are somewhat richer in peaks and certainly reflect possible precipitation of organic species on the electrodes' surface. Note the peak around 1830 cm^{-1} in the spectrum of the electrode cycled in the VC-containing solution (Fig. 11c), which may reflect formation of polycarbonate due to oxidative polymerization of VC. The spectrum of the electrode cycled in the solution containing AD25 (Fig. 11d) is rich in peaks around 1600-1800 cm^{-1}, correlating with the Fig. 10c spectrum above, and may reflect precipitation of derivatives of salicylic acid on the electrode's surface. These spectra, measured by the diffuse reflectance mode from powders scraped from the electrodes, can never be obtained at a high enough resolution for a rigorous identification of surface species. However, they definitely reflect that these electrodes interact with solution species. The presence of the additives definitely influences their surface chemistry. Hence, we propose that the performance of the $LiMn_2O_4$ cathodes also depends on surface phenomena such as surface film formation. The VC and AD25 additives that were found to have a pronounced impact on the surface chemistry and performance of the negative (C-Li) electrodes, also affect the behavior of $LiMn_2O_4$ cathodes by influencing their surface chemistry (probably via precipitation of surface films). This explains the difference in the electrochemical behavior of $LiMn_2O_4$ electrodes (CV, EIS, galvanostatic cycling) in the three solutions, and demonstrates the ability to influence the performance of the cathodes by a small amount of filming additives in solutions.

Figure 12 compares XPS spectra of Pt electrodes polarized to 4.5 V (Li/Li^+) in the three solutions, as indicated. The spectra show a wide range of binding energy, and reflect the formation of surface species containing carbon, oxygen, and fluorine, as expected. We do not deal herein with details regarding the F, O, and C peaks of these spectra. There are two major results that should be emphasized:

1. The platinum peaks are clearly seen in the spectra of the electrodes treated in additive-free and VC solutions, but are absent in the spectra related to the solution containing AD25.

2. The fluorine peak is much smaller and the carbon peak is higher in the spectrum related to the AD25 solutions, compared to the other two spectra of Fig. 12.

This presents evidence of the high surface activity of AD25 and the formation of surface films, which suppressed other possible sur-

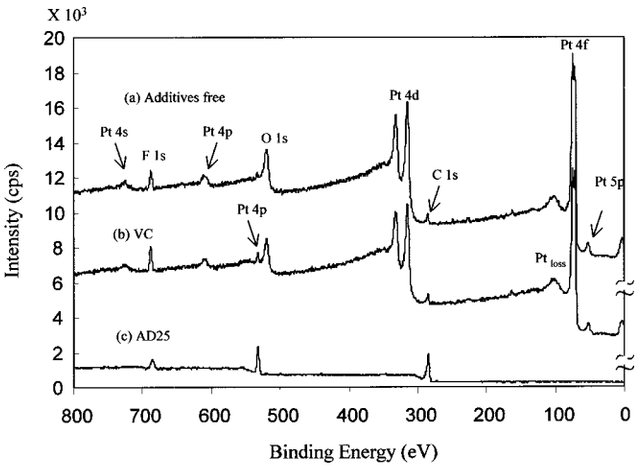

Figure 12. XPS data obtained from Pt electrodes polarized anodically to 4.5 V (for 3 h) in EC:DEC:DMC, 1 M (a) LiFAP, (b) LiFAP + 5% VC, and (c) LiFAP + 1% AD25 solutions as indicated.

face reactions (*e.g.*, those connected with the salt anion). These XPS data correlate with the FTIR spectra of Fig. 10 and 11, which also reflect a pronounced surface activity of AD25 at high potentials.

Conclusion

The new salt from Merck, $LiPF_3(CF_2CF_3)_3$ (LiFAP) can be considered as a good replacement for $LiPF_6$ in electrolyte solutions for Li-ion batteries. Both graphite and $LiMn_2O_4$ electrodes behaved reversibly in LiFAP solutions, better than in $LiPF_6$ solutions in similar experiments and under similar conditions, as already discussed.[22] In this work we went one step further with the examination of this new salt, by testing its solutions with two additives, vinylene carbonate (VC) and Li *bis* (salicylatoborate) (AD25). It should be emphasized that even if these additives were already examined in $LiPF_6$ solutions,[34] the results cannot be relevant for other salt solutions because of the complexity of the electrodes' surface chemistry that determines their performance.

The surface chemistry of both Li-C and $LiMn_2O_4$ electrodes depended on the interrelation among the surface reactions of the salt anion, solvent molecules, and additives. Both VC and AD25 reacted predominantly on the Li-C and $LiMn_2O_4$ electrode surfaces in spite of the high reactivity of the alkyl carbonate solvents. Because the surface chemistry is complicated, as it is affected by all solution components, it was impossible to identify precisely the reaction products of the additives on the electrodes' surface using FTIR and XPS, which are the surface techniques available to us for specific identification of surface species. However, it can be suggested that, based on the spectral studies, VC was reduced to species such as poly-Li alkyl carbonate, $ROCO_2Li$ species, and polycarbonates. AD25 was reduced to species with carboxylate groups, VC was oxidized to polycarbonates, and AD25 was oxidized to species with ester and/or anhydride groups.

The above surface reactions considerably influence the electrochemical behavior of the electrodes, as measured by voltammetry, impedance spectroscopy, and repeated (cycling) chronopotentiometry. VC was proven to be a desirable additive that improved the behavior of both Li graphite and $LiMn_2O_4$ electrodes, especially at elevated temperatures, in terms of reversibility and stability. LiFAP solutions with AD25 were found to be inferior to VC- and additive-free solutions for use with Li graphite and $LiMn_2O_4$ electrodes. We suggest that the presence of VC improved the performance of Li-graphite anodes because the polymeric species containing OCO_2Li groups are formed by VC reduction, which improves both passivation and Li-ion transport through the surface films (from EIS). In addition, VC polymerization on $LiMn_2O_4$ may reduce detrimental interactions of this material with the solutions (*e.g.*, reactions with trace acidic species, which lead to Mn dissolution).

This work demonstrates that it is possible to improve considerably the performance of Li-ion battery systems by the use of additives in solutions at relatively low concentrations (a few percents) that react predominantly on the electrode surfaces and improves their passivation.

Acknowledgments

Partial support for this work was obtained from the BMBF, the German Ministry of Science, in the framework of the DIP program for Collaboration between Israeli and German Scientists.

One of the authors, D. Aurbach, assisted in meeting the publication costs of this article.

References

1. J. M. Tarascon and M. Armand, *Nature (London)*, **414**, 359 (2001).
2. S. S. Zhang, M. S. Ding, K. Xu, J. Allen, and T. R. Jow, *Electrochem. Solid-State Lett.*, **4**, A206 (2001).
3. D. Aurbach, *J. Power Sources*, **89**, 206 (2000).
4. T. Eriksson, A. M. Andersson, A. G. Bishop, C. Gejke, T. Gustafsson, and J. O. Thomas, *J. Electrochem. Soc.*, **149**, A69 (2002).
5. K. Kanamura, H. Tamura, and Z. Takehara, *J. Electroanal. Chem.*, **333**, 127 (1992).
6. D. Aurbach, K. Gamolsky, B. Markovsky, G. Salitra, and Y. Gofer, *J. Electrochem. Soc.*, **147**, 1322 (2000).
7. M. M. Thackeray, *Prog. Solid State Chem.*, **25**, 1 (1997).
8. A. Yamada and S. C. Chung, *J. Electrochem. Soc.*, **148**, A960 (2001).
9. J. Cho and M. M. Thackeray, *J. Electrochem. Soc.*, **146**, 3577 (1999).
10. G. Amatucci, A. D. Pasquier, A. Blyr, T. Zheng, and J.-M. Tarascon, *Electrochim. Acta*, **45**, 255 (1999).
11. Y. Xia, Y. Zhou, and M. Yoshio, *J. Electrochem. Soc.*, **144**, 2593 (1997).
12. S. J. Wen, T. J. Richardson, L. Ma, K. A. Striebel, P. N. Ross, and E. J. Cairns, *J. Electrochem. Soc.*, **143**, L136 (1996).
13. X. Wang, K. Yasukawa, and S. Mori, *Electrochim. Acta*, **45**, 2677 (2000).
14. M. Morita, T. Shibata, N. Yoshimoto, and M. Ishikawa, *Electrochim. Acta*, **47**, 2787 (2002).
15. W. Xu and C. A. Angell, *Electrochem. Solid-State Lett.*, **4**, E1 (2001).
16. K. Xu, S. Zhang, T. R. Jow, W. Xu, and C. A. Angell, *Electrochem. Solid-State Lett.*, **5**, A26 (2002).
17. D. Aurbach, Y. Ein-Eli, B. Markovsky, Y. Carmeli, H. Yamin, and S. Luski, *Electrochim. Acta*, **39**, 2559 (1994).
18. Y. Ein-Eli, S. R. Thomas, and V. R. Koch, *J. Electrochem. Soc.*, **144**, 1159 (1997).
19. G. H. Wrodnigg, J. O. Besenhard, and M. Winter, *J. Electrochem. Soc.*, **146**, 470 (1999).
20. C. Jehoulet, P. Biensan, J. M. Bodet, M. Broussely, C. Moteau, and C. T. Lescourret, in *Batteries for Portable Applications and Electric Vehicles*, C. F. Holmes and A. R. Landgrebe, Editors, PV 97-18, p. 974, The Electrochemical Society Proceedings Series, Pennington, NJ (1997).
21. M. Schmidt, U. Heider, A. Kuehner, R. Oesten, M. Jungnitz, N. Ignatev, and P. Sartori, *J. Power Sources*, **97-98**, 557 (2001).
22. J. S. Gnanaraj, M. D. Levi, Y. Gofer, D. Aurbach, and M. Schmidt, *J. Electrochem. Soc.*, **150**, A445 (2003).
23. A. Martinent, B. L. Gorrec, C. Montella, and R. Yazami, *J. Power Sources*, **97-98**, 83 (2001).
24. D. Aurbach and Y. Gofer, *J. Electrochem. Soc.*, **138**, 3529 (1991).
25. M. D. Levi and D. Aurbach, *J. Phys. Chem. B*, **101**, 4641 (1997); M. D. Levi and D. Aurbach, *J. Phys. Chem. B*, **101**, 4630 (1997).
26. J. S. Gnanaraj, M. D. Levi, E. Levi, G. Salitra, D. Aurbach, J. F. Fischer, and A. Claye, *J. Electrochem. Soc.*, **148**, A525 (2001).
27. D. Aurbach, K. Gamolsky, B. Markovsky, and Y. Gofer, *Electrochim. Acta*, **47**, 1423 (2002).
28. D. Aurbach, B. Markovsky, K. Gamolsky, E. Levi, and Y. Ein-Eli, *Electrochim. Acta*, **45**, 67 (1999).
29. D. Aurbach, B. Markovsky, A. Schechter, Y. Ein-Eli, and H. Cohen, *J. Electrochem. Soc.*, **143**, 3809 (1996).
30. C. J. Puchert, *Aldrich Library of FTIR Spectra*, 1st ed., Vol. 1 and 2, Aldrich Chemical Co., Ltd., Milwaukee, WI (1980).
31. D. Aurbach, M. D. Levi, E. Levi, H. Teller, B. Markovsky, G. Salitra, L. Heider, and U. Heider, *J. Electrochem. Soc.*, **145**, 3024 (1998).
32. D. Aurbach, B. Markovsky, M. D. Levi, E. Levi, A. Schechter, M. Moshkovich, and Y. Cohen, *J. Power Sources*, **81-82**, 95 (1999).
33. T. Eriksson, A. M. Andersson, C. Gejke, T. Gustafsson, and J. O. Thomas, *Langmuir*, **18**, 3609 (2002).
34. D. Aurbach, B. Markovsky, A. Rodkin, E. Levi, Y. S. Cohen, H.-J. Kim, and M. Schmidt, *Electrochim. Acta*, **47**, 4291 (2002).